Lawrence Berkeley National Laboratory
Recent Work

Title
THE CHEMICAL COMPOSITION OF PRECIPITATED AUSTENITE IN 9Ni STEELS

Permalink
https://escholarship.org/uc/item/2h9492kf

Author
Fultz, B.

Publication Date
1985-07-01

Lawrence Berkeley Laboratory
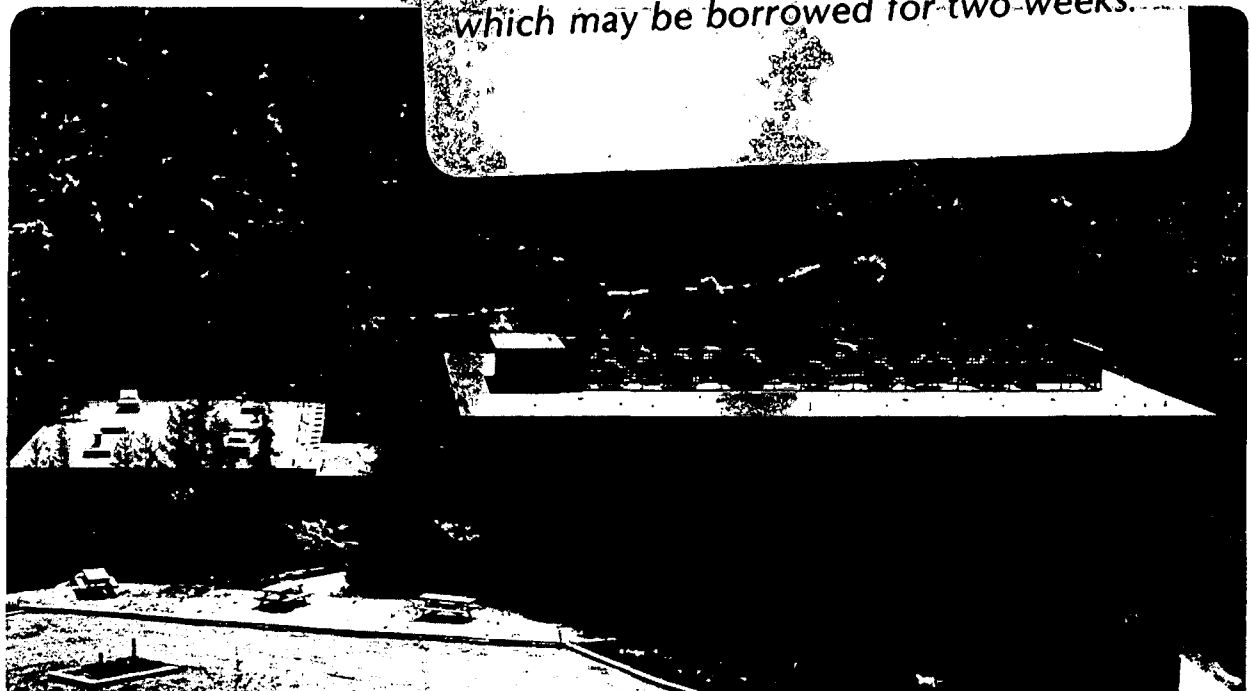## UNIVERSITY OF CALIFORNIA

Materials & Molecular Research Division

THE CHEMICAL COMPOSITION OF PRECIPITATED
AUSTENITE IN 9Ni STEELS

B. Fultz, J.I. Kim, and Y.H. Kim,
and J.W. Morris, Jr.

July 1985

LBL-19938

DISCLAIMER

The Chemical Composition of Precipitated Austenite in 9Ni Steel

B. Fultz*, J. I. Kim†, Y. H. Kim† and J. W. Morris, Jr.

Dept. of Materials Science and Mineral Engineering, Univ. of Calif. and the

Lawrence Berkeley Laboratory, Berkeley, Calif. 94720.

* Present address: Keck Laboratory, California Institute of Technology, Pasadena, Calif. 91125.

† Present address: IBM Thomas J. Watson Research Center, Yorktown Heights, New York 10598.

ABSTRACT

Analytical scanning transmission electron microscopy and a novel Mössbauer spectrometry technique were used to measure the chemical composition of austenite particles which precipitate during intercritical tempering of 9Ni steel. Both techniques showed an enrichment of Ni, Mn, Cr and Si in the austenite. A straightforward analysis involving data on both austenite composition and austenite formation kinetics suggests that the growth of austenite particles is controlled by a 3-dimensional diffusion process. The segregation of solutes to the austenite accounts for much of its stability against the martensitic transformation. Composition inhomogeneities develop in austenite particles after long temperings; the central regions of the particles are lean in solutes and are first to undergo the martensitic transformation. However, changes in solute concentrations of the austenite during long temperings seem too small to account for the large changes in austenite stability. It appears that some of the stability of precipitated austenite is microstructural in origin.

INTRODUCTION

Commercial 9Ni steel is prepared for service at cryogenic temperatures by an intercritical tempering which forms small fcc austenite particles within the bcc martensite matrix. The cryogenic toughness of 9Ni steel requires not only the presence of austenite, but also a certain degree of stability of the austenite particles against the fcc→bcc martensitic transformation. Correlations between the stability of austenite particles and the cryogenic toughness of 9Ni steel are well-established [1,2,3]. The austenite particles are expected to be thermodynamically unstable against the fcc→bcc martensitic transformation, however, so their resistance to transformation is a question of fundamental as well as of practical interest.

Equilibrium phase diagrams suggest that a segregation of Ni, Mn, Cr or C to the austenite particles during intercritical tempering could be responsible for some of the austenite stability. Unfortunately, it is difficult to measure the solute concentration of austenite particles because they are so small, having dimensions of only a few hundred Å in the early stages of intercritical tempering [4]. Modern experimental techniques are required for these composition measurements, and here we report data obtained by analytical scanning transmission electron microscopy (STEM) and by transmission Mössbauer spectrometry (TMS). A dramatic reduction in the austenite stability occurs as intercritical tempering proceeds [1], and this change in austenite stability with tempering time poses a well-defined problem for laboratory investigation. We sought to determine how much of this change in austenite stability during tempering is attributable to composition changes of the austenite particles. In addition, an analysis of both the amount of austenite and its solute composition provides basic information about how the austenite particles are formed during intercritical tempering.

EXPERIMENTAL PROCEDURES and DATA ANALYSIS

Commercial 9Ni steel plates were kindly supplied by the Nippon Kokan Company, and were prepared as described previously [1]. The chemical composition of this material was (in wt.%): 9.1 Ni, 0.50 Mn, 0.20 Si, 0.17 Cr, 0.08 C, 0.004 P, 0.004 S with a balance of Fe. Intercritical tempering was performed at 590°C for times ranging from 0.8 to 627 hrs. Specimens for study by STEM and TMS were prepared from wafers cut from bulk material with an abrasive saw under flood cooling. These wafers were thinned in a solution of 3% HF, 29% H_2O_2 and 68% H_2O to a thickness of approximately 35 μm for TMS, and 100 μm for further preparation for STEM. The chemically-thinned wafers for STEM were spark-cut into disks of 3 mm diameter, which were ground to a thickness of 50 μm. The disks were then thinned to perforation in a twin-jet electro-polishing apparatus using a cooled solution of 400 ml CH_3COOH, 75 gm CrO_3 and 30 ml H_2O.

Analytical STEM measurements employed a Phillips 400ST electron microscope operated at 120 keV with a 20 Å probe size. X-ray fluorescence from the specimen was measured by a Si detector with a 0.2 μm dead layer mounted behind a 0.6 μm Be window. The detector take-off angle was 25° and the specimen tilting angle was 20°. The Kα x-ray peak for each element was first corrected for the gradual background intensity, and was then corrected for extraneous x-ray flourescence in the microscope. The latter correction was performed for each element by subtracting a hole count that was scaled by the intensity of the Cu Kα peak in the observed spectrum. Integrated intensities of x-ray peaks were converted into chemical concentrations with proportionality constants invol-ving the detector characteristics, and the ionization and fluorescence characteristics of the elements [5,6]. Relative errors of about ±15% in these corrections and conversions are expected, but these are systematic errors that will be the same for all specimens. We were more concerned that the probe beam could analyze material on both sides of the austenite-martensite interface. Care was taken to ensure that the probe beam did not intersect a sloping austenite-martensite interface, and the

intrinsic beam broadening in our specimens was checked by moving the probe beam across a sharp austenite-martensite interface.

The lack of hyperfine structure in the Mössbauer peak of the austenite phase precluded its use for measuring the austenite solute composition. Instead, the average chemical composition of the austenite was determined from measurements of the amount of austenite together with changes in the solute concentration of the martensite. It is straightforward to determine the amount of austenite in 9Ni steel by taking the ratio of the the austenite peak intensity to the total intensity of the Mössbauer spectrum [7,8], but determining changes in the solute concentration of the martensite required substantial development work [9-11]. Chemical information is obtained by analysis of the ^{57}Fe hyperfine magnetic field distribution. In the bcc martensite of 9Ni steel, solute atoms situated near ^{57}Fe atoms perturb the ^{57}Fe hyperfine magnetic fields through three mechanisms [12,13]. 1) The magnetic moments at Ni, Mn, Cr and Si atoms are substantially smaller than the moments at Fe atoms, and the 4s conduction electron spin density is redistributed around these solutes in a way that reduces the hyperfine magnetic field at ^{57}Fe atoms with solute atoms as first or second nearest neighbors. 2) Magnetic moments at ^{57}Fe atoms are increased when Ni atoms are nearby, and this causes the ^{57}Fe hyperfine magnetic field to increase. 3) When Ni atoms increase magnetic moments at Fe atoms which are also first or second nearest neighbors of a ^{57}Fe atom, the ^{57}Fe hyperfine magnetic field will increase due to a 4s spin density redistribution around these Fe atoms.

Details of how these three mechanisms contribute to the full hyperfine magnetic field distribution as measured by Mössbauer spectrometry cannot be fully described here, but the general systematics turn out to be fairly simple [11]. Mn, Cr and Si atoms perturb the ^{57}Fe hyperfine magnetic field primarily through mechanism 1 [12], so ^{57}Fe atoms with Mn, Cr or Si neighbors contribute to distinct satellite peaks on the *low* energy sides of the six absorption peaks from the martensite. Because mechanism 1 involves the first and second bcc nearest neighbor shells, the fraction of intensity in these satellites is approximately 14 times the combined concentration of Mn, Cr and Si

[11]. All three types of ^{57}Fe hyperfine magnetic field perturbations are important for Ni solutes [12], and at room temperature they cause an increased absorption on the *high* energy side of the six martensite peaks. Empirical calibrations with Fe-Ni alloys of known composition were developed [11], and changes in the intensity on the high energy side of Mössbauer peaks after tempering were linearly related to changes in the Ni concentration of the martensite.

RESULTS

Measurements of the chemical composition of precipitated austenite as a function of tempering time are presented in Fig. 1. Both the STEM and TMS data of Fig. 1A show an enriched Ni concentration in the austenite which reaches 15% after long tempering times. Fig. 2 shows a sequence of differences between TMS spectra taken before and after tempering from 1 hr to 81 hrs. The TMS data are less reliable for short tempering times because both the intensity of the austenite peak (in the center of the spectrum) and the difference intensity due to the loss of solutes in the martensite (on the low and high energy sides of martensite peaks nos. 1 and 6) are weak. Broadening of the STEM probe beam caused errors in the solute concentration of the austenite during the early stages of intercritical tempering when the austenite particles had dimensions less than 0.1 μm [1]. However, from the sharpness of the Ni concentration gradient measured at the austenite-martensite interface (Fig. 3), we deduce that most of the increase in Ni concentration of the austenite during tempering is real, and not due to a reduction in beam broadening effects as the particles grow larger. We believe that the STEM data show the correct trend of an increasing Ni concentration in the austenite with tempering time.

The combined concentrations of Mn, Cr and Si in the austenite are presented as a function of tempering time in Fig. 1B. For these solutes the TMS data are more reliable than the STEM data. X-ray fluorescence peaks from these elements were quite weak, and the background and hole count

corrections were large. Fig. 1C shows the C concentration of the austenite as a function of tempering time. These data were obtained from the x-ray lattice parameter of the austenite [1]. In preparing Fig. 1C, the analyses of austenite and martensite lattice parameters were averaged for the longer tempering times. It was assumed that the martensite C concentration was depleted after 10 hrs. of intercritical tempering, since the martensite lattice parameter remained unchanged after this time.

Conventional TEM bright field and dark field micrographs of 9Ni steel tempered for 81 hrs are shown in Fig. 4. Although the austenite particles did not transform to martensite in bulk sections of this material [1], during the preparation of thin foils some austenite particles began to transform. The central parts of several particles in Fig. 4 did not contribute to the (002)fcc diffraction because they had transformed to martensite. Unfortunately, selected area diffraction patterns were not obtained from the central parts of the partially transformed particles, but their sharp delineation and the defect structures in them are strong evidence that they are indeed bcc martensite. In addition, dislocation structures in the surrounding tempered martensite matrix, attributable to the large transformation strains [14], are evident in Fig. 4.

DISCUSSION

We can determine the type of diffusion process which controls the growth of austenite particles by considering both the austenite solute concentration and the rate of austenite formation. For the first 27 hrs of tempering, the volume fraction of austenite increases as $t^{0.45}$ [1]. This increase is due to the growth of existing particles rather than the nucleation of new particles [1], so the volume of each austenite particle increases as $t^{0.45}$. Naïvely this seems consistent with the $t^{0.5}$ growth rate which occurs when precipitate growth is controlled by a 1-dimensional diffusion process, and the precipitate forms with a constant solute composition. However, to determine the geometry of the

controlling diffusion process, it is necessary to explicitly consider the changes in the solute concentration of the austenite. For simplicity we consider only the enrichment of Ni, $\Delta c(t)$, because Ni is the major solute in the austenite and is also the slowest diffusing species.

$$\Delta c(t) \equiv c_{Ni}(t) - c_o \quad ,$$

where c_0 is the initial Ni concentration of the martensite. The change in volume of an austenite particle, ΔV, depends on the inverse of $\Delta c(t)$ because the larger the required solute enrichment, the smaller will be the increase in ΔV during the time interval Δt :

$$\Delta V = \frac{c_o}{\Delta c(t)} \left(\sqrt{2D \cdot (t + \Delta t)}^N - \sqrt{2D \cdot t}^N \right) .$$

Here N, which we hope to determine, is the dimensionality of the growth-controlling diffusion process and D is the diffusivity of Ni. We use the binomial approximation and find:

$$V(t) = c_o N D^{N/2} \int_0^t \frac{(2t')^{N/2 - 1}}{\Delta c(t')} dt' \quad .$$

A simple linear dependence of $\Delta c(t)$ on t is probably all that can be justified by the data of Fig. 1A. Since V increases approximately as $t^{0.5}$, the value of N must be 3. The growth of austenite particles appears to be controlled by a 3-dimensional mechanism of diffusional growth. The data of Fig 1A may also allow that $\Delta c(t)$ increases as $t^{0.5}$, so the growth of austenite particles may be controlled by a 2-dimensional diffusion process, or a mixture of a 3-dimensional process with a process of lower dimensionality. Note, however, that a 1-dimensional diffusion process requires that $\Delta c(t)$ is independent of t, contrary to our most reliable experimental data.

We propose that austenite particles form on martensite lath boundaries and on prior austenite grain boundaries [4] only because these are low energy sites for nucleation. Sometimes precipitates form on grain boundaries because solutes diffuse to the nearest grain boundary by a slow bulk diffusion mechanism, and are then rapidly swept to the growing precipitate by a grain boundary diffusion mechanism. However in the early stages of such a precipitation process, the diffusion of solutes to the nearest grain boundary will be a 1-dimensional process, which is inconsistent with the previous analysis.

We propose that the Ni concentration of precipitated austenite changes with tempering time because of changes in the C concentration of the austenite. Carbon is a rapidly diffusing species, so at 590°C the carbon distribution in both the austenite and the martensite is able to satisfy the requirements of chemical equilibrium. However after about 10 hrs of tempering, essentially all of the carbon has segregated to the austenite. Since the austenite particles continue to grow, they must do so with a reduced C concentration. The continued growth of austenite particles then requires a progressively greater segregation of Ni, as shown by the STEM data of Fig. 1A. The diffusivity of Ni in austenite is quite small at 590°C, so the Ni concentration in the austenite will not homogenize. A Ni concentration gradient in the austenite particles is therefore expected. The centers of the particles, which formed when the carbon concentration was highest, will have the lowest Ni concentration. The outer parts of the particle, which formed when the carbon concentration was lowest, will have the highest Ni concentration. This is just the Ni concentration profile which is seen in Fig. 3 *. With their reduced Ni concentrations, the centers of austenite particles will be the first regions to undergo the martensitic transformation, and this is seen in Fig. 4.

---

* Carbon is quite mobile in austenite at 590°C, so it will distribute homogeneously throughout the austenite particles.

We interpret M_S (the temperature at which the precipitated austenite begins to spontaneously transform to martensite) in terms of the austenite composition using the relation [15]:

$$M_S(°C) = 561 - 474\ \%C - 33\ \%Mn - 17\ \%Ni - 17\ \%Cr\ ,$$

with concentrations in wt.%. Using data of Fig. 1, we estimate that the precipitated austenite in material tempered for 1 hr has an M_S of about 70°C. The suppression of M_S from 561 to 70°C is substantial, so the solute concentration of the austenite is a major factor contributing to the austenite stability. However, the austenite formed after a 1 hr tempering is not only stable at 70°C, but also at -196°C, and it is even mechanically stable at room temperature [1]. Not all of this stability seems attributable to solute enrichment. Furthermore, the changes in austenite chemistry between 1 and 100 hrs of tempering (a decrease in C concentration and an increase in Ni concentration) should cause M_S to increase by only 40 to 50°C. The observed increase in M_S between 1 and 100 hrs of tempering is greater than 200°C [1], so the changes in austenite composition during tempering make only a small contribution to the decrease in austenite stability. Factors other than chemical composition evidently contribute to the stability of precipitated austenite in 9Ni steel. These other factors are presumed to be microstructural in their origin. In a recent publication [14], we have described a mechanism by which changes in dislocation structures around transformed austenite particles cause a reduction in mechanical stability of precipitated austenite during isothermal tempering.

SUMMARY and CONCLUSIONS

The growth of austenite particles in 9Ni steel during intercritical tempering at 590°C is controlled by bulk diffusion in the bcc martensite phase. The solutes apparently reach the growing austenite particles by diffusing radially inwards towards them, and not by short-circuit, high diffusivity paths. It seems that austenite particles form on martensite lath boundaries and on prior austenite grain boundaries because they are low energy sites for nucleation. Carbon diffuses rapidly to austenite particles, and in about 10 hrs the austenite has consumed all of the carbon in the martensite. Austenite particles then continue to grow with a reduced carbon concentration, but an increased nickel concentration. Because of its low diffusivity in austenite, Ni remains concentrated in the outer regions of austenite particles, which are the last to form. The outer regions are therefore most stable against the martensitic transformation, and it was observed that the centers of austenite particles tended to be first to transform.

Analytical STEM, transmission Mössbauer spectrometry and x-ray diffractometry measurements showed substantial enrichments of Ni, Mn, Cr, Si and C in the austenite particles. These solute enrichments are a major factor contributing to the low M_s of the particles, but they do not account for all of the austenite stability. Even more significant is the discrepancy between the large change in austenite stability with tempering time and the relatively small changes in Ni and C concentrations of the austenite. For these reasons we propose that the stability of the precipitated austenite in 9Ni steel has a microstructural, in addition to a chemical origin.

ACKNOWLEDGEMENTS

REFERENCES

1. B. Fultz, J. I. Kim, Y. H. Kim, H. J. Kim, G. O. Fior and J. W. Morris, Jr.: *Metall. Trans. A*, in press.

2. K. J. Kim and L. H. Schwartz: *Mater. Sci. Eng.*, 1978, vol. 33, p. 5-20.

3. C. W. Marschall, R. F. Heheman and A. R. Troiano: *Trans. ASM*, 1962, vol. 55, p. 135-148.

4. C. K. Syn, B. Fultz and J. W. Morris, Jr.: *Metall. Trans.*, 1978, vol. 9A, p. 1635-1640.

5. N. J. Zaluzec: *Introduction to Analytical Microscopy*, p. 121, Plenum, New York, 1979.

6. G. Cliff and G. W. Lorimer: *J. Microscopy*, 1975, vol. 103, p. 203.

7. L. H. Schwartz: *Applications of Mössbauer Spectroscopy, Vol. I*, p. 62, Academic Press, New York, 1976.

8. H. L. Marcus, L. H. Schwartz and M. E. Fine: *Trans. ASM*, 1966, vol. 59, p. 468.

9. B. Fultz and J. W. Morris, Jr.: *Nuclear and Electron Resonance Spectroscopies Applied to Materials Science*, p. 377, Elsevier North Holland, New York, 1981.

10. B. Fultz and J. W. Morris, Jr.: University of Calif. and the Lawrence Berkeley Laboratory, unpublished research, 1985.

11. B. Fultz and J. W. Morris, Jr.: *Industrial Applications of the Mössbauer Effect*, Plenum, New York, in press.

12. M. B. Stearns: *Phys. Rev. B.*, 1976, vol. 13, pp. 1183-1197.

13. M. B. Stearns: *Phys. Rev. B.*, 1974, vol. 9, pp. 2311-2327.

14. B. Fultz and J. W. Morris, Jr.: *Metall. Trans. A*, in press.

15. E. C. Bain and H. W. Paxton: *Alloying Elements in Steel*, 2nd ed., p. 266, ASM, Metals Park, 1966.
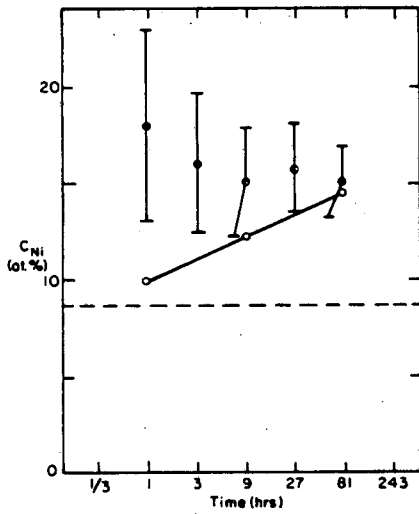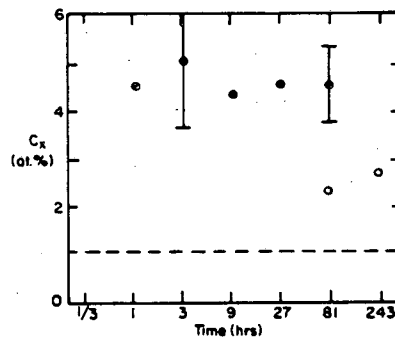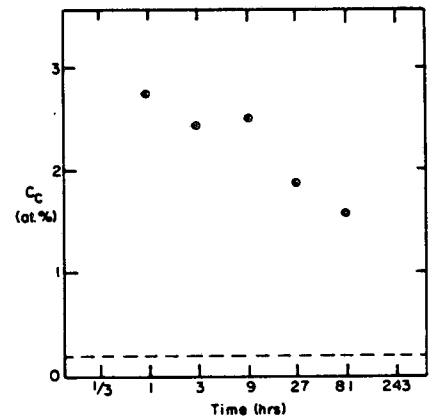
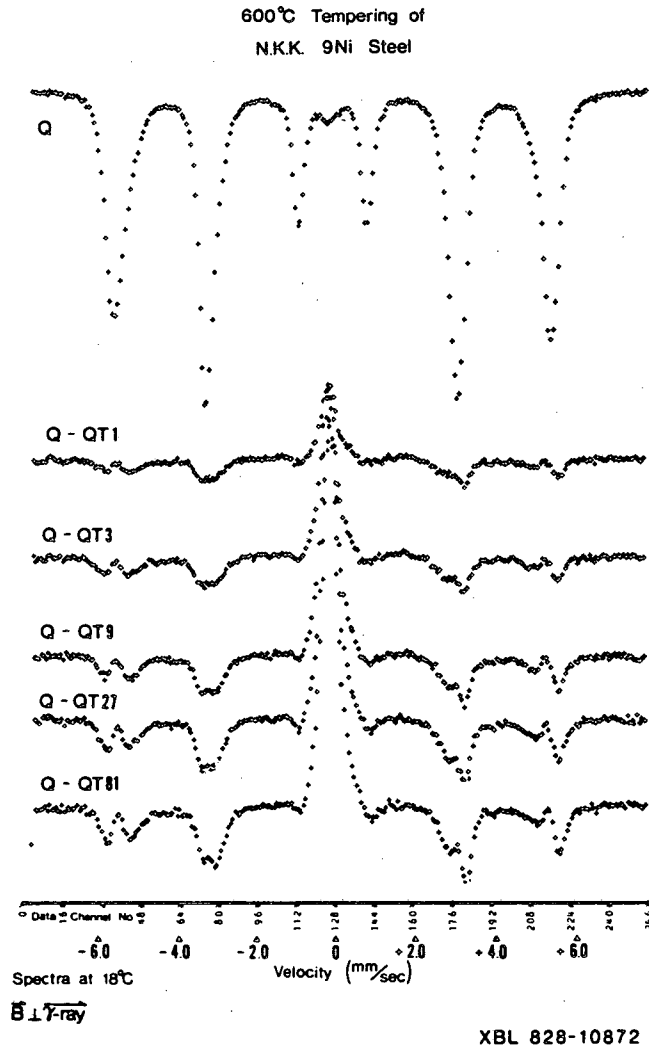1. Solute concentrations of the austenite versus tempering time at 590°C.

A: Ni concentration; B: Mn, Cr and Si combined concentration; C: C concentration from x-ray

lattice parameters. A and B: TMS data are solid points, analytical STEM data are open points.

Dashed lines show average concentration in the alloy.

600°C Tempering of
N.K.K. 9Ni Steel

Q

Q - QT1

Q - QT3

Q - QT9

Q - QT27

Q - QT81

-6.0   -4.0   -2.0   0   +2.0   +4.0   +6.0
Velocity (mm/sec)

Spectra at 18°C

B⊥ɣ-ray

XBL 828-10872

2. Mössbauer difference spectra from 9Ni steel taken at 18°C after temperings at 590°C. The spectrum from untempered material is shown at the top. TMS spectra from tempered materials are not shown; instead the differences between spectra of untempered material and material tempered from 1 to 81 hrs are shown. The minuend and subtrahend were normalized so that martensite peaks no. 1 had the same dip.
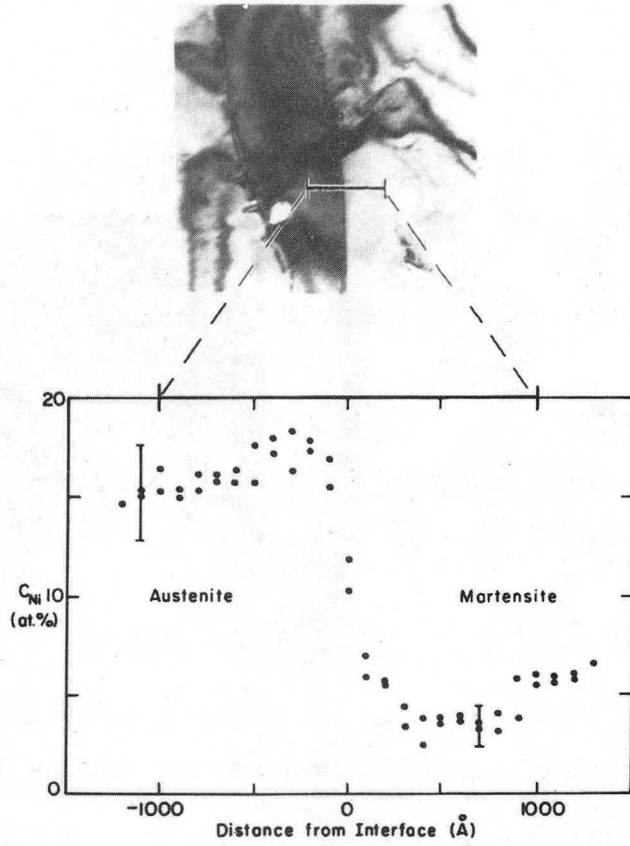
XBB 857-5318

3. Analytical STEM data of a Ni concentration profile across an austenite-martensite interface. The data of the lower graph were taken along the line shown in the TEM bright field micrograph at top.

XBB 857-5221

4. Left: TEM bright field micrograph of 9Ni steel tempered for 81 hrs. Right: Complementary

TEM dark field micrograph from the (002)fcc diffraction with zone condition: [111]bcc ∥ [110]fcc .

LAWRENCE BERKELEY LABORATORY
TECHNICAL INFORMATION DEPARTMENT
UNIVERSITY OF CALIFORNIA
BERKELEY, CALIFORNIA 94720